

Strangeness and threshold of phase changes

Johann Rafelski¹, Inga Kuznetsova¹, and Jean Letessier^{1,2}

¹ Department of Physics, University of Arizona, Tucson, AZ 85721

² LPTHE, Université Paris 7, 2 place Jussieu, F-75251 Cedex 05

E-mail: rafelski@physics.arizona.edu

Abstract. We explore entropy and strangeness as signature of QGP for top AGS and the energy scan at SPS. We find that the hadronization dynamics changes between 20 and 30 A GeV projectile energy. The high energy results are consistent with QGP.

PACS numbers: 24.10.Pa, 25.75.-q, 13.60.Rj, 12.38.Mh

1. Introduction

It is commonly accepted that, at RHIC, we have produced the quark-gluon plasma (QGP) in laboratory; the question is if this new state of matter is already present in the SPS energy range as has been considered likely in the CERN press release of February 2000? We present here a brief discussion of our findings as described in full length elsewhere [1, 2]. Here, we look at the abundant production of strange flavored hadrons in the relativistic heavy ion collisions at top AGS and all SPS energies, addressing the NA49 energy scan results [3].

Our data analysis employs the statistical hadronization model (SHM); we assume that the strong interactions saturate the quantum particle production matrix elements. Therefore, the yield of particles is controlled dominantly by the magnitude of the accessible phase space. The SHM contains little if any information about the nature of interactions, and thus, it embodies the objective of reaching simplicity in many body dynamics, allowing to identify the properties of the dense and hot primary matter formed in heavy ion collisions. Interpretation of experimental data is arrived at with the SHARE suite of programs [4].

2. Strangeness and Entropy

The total final state hadron multiplicity is a measure of the entropy S produced. In the QGP, the entropy production occurs predominantly early on in the collision, once a quasi-thermal exponential energy distribution of partons has been formed, the entropy production has been mostly completed, even if the chemical yield equilibrium is not achieved yet. Since the kinetic processes leading to strangeness production are slower

than the parton equilibration process, we are rather certain that the production of entropy occurs mainly prior to strangeness production. Even though the degree of chemical equilibration of gluons in early stages (which dominate strangeness production) are uncertain, study of kinetic strangeness production show that the controlling quantity is the entropy contents. For this reason, the observable ‘strangeness pairs per entropy’ N_s/S (also colloquially referred to as s/S) emerges as diagnostic tool, also since in essence both s and S are conserved in the process of hadronization.

The phase space density is in general different in any two matter phases. Thus when transformation of one phase ‘Q’ (for QGP) into the other occurs rapidly, given chemical equilibrium in the decaying phase, in general the final state is out-of-chemical equilibrium. Especially, when hadrons are produced in a recombinant model, in order to preserve entropy, there must be a jump in the phase space occupancy parameters $\gamma_i^Q < \gamma_i$, $i = q, s$. The superscript Q indicates that we refer to the QGP phase; variables in the hadron phase will be stated without an superscript.

This jump replaces the increase in volume found in a slow transformation involving re-equilibration. In order to preserve entropy in sudden hadronization of supercooled QGP at $T \simeq 140$ MeV, we must have for the light quark ‘q’ occupancy $\gamma_q^{\text{cr}} = e^{m_\pi/T}$. The value γ_q^{cr} is where the pion gas condenses. The required value of γ_q is decreasing with increasing temperature and is crossing $\gamma_q = 1$ near $T \simeq 180$ MeV. Thus, in fast hadronization of the QGP phase (without an increase in volume, i.e., mixed phase), we expect that, the value of γ_q governing hadron yields must be greater than unity for every value of T considered in previous studies of the hadronization process, with the relation being approximately as $\gamma_q \simeq 1.6 - 0.015(T - 140)$ [MeV].

The ratio s/S up to a structural numerical factor compares the degeneracy of strangeness to the overall QGP effective degeneracy. At sufficiently high temperature, the entropy density S/V in QGP is that of (nearly) ideal quark-gluon gas:

$$\frac{S}{V} = \frac{4\pi^2}{90} g_{\text{eff}}^Q(T) T^3 = \text{Const.}, \quad (1)$$

For an equilibrated QGP phase with perturbative properties:

$$\frac{s}{S} \equiv \frac{\rho_s}{S/V} \simeq \frac{(\gamma_s^Q(t) g_s^Q / \pi^2) T^3 0.5 x^2 K_2(x)}{g_{\text{eff}}^Q 4\pi^2 / 90 T^3} = \frac{\gamma_s^Q g_s^Q}{g_{\text{eff}}^Q} 0.23 [0.5 x^2 K_2(x)]. \quad (2)$$

For early times, when $x = m_s/T(t)$ is relatively small, assuming the equilibrium value ($\gamma_s^Q = 1$), we can find $s/S \simeq 0.045$. However, at high temperature strangeness is not yet equilibrated chemically and in general the value in QGP at hadronization is expected in the range $0.03 < s/S < 0.04$. When and if strangeness is not equilibrated in the QGP source, we in effect can determine the value γ_s^Q by comparing to the above expectations.

In order to arrive at the above estimate, we needed to use the number of degrees of freedom in chemically equilibrated QGP, which is shown by dashed lines in Fig. 1. Solid lines allow for the effect of approach to chemical equilibrium of strangeness, assuming: $\gamma_s^Q \simeq (300 - T)/160$ MeV. Most of temperature dependent corrections cancel, and one finds in the latter case that it is possible to use a nearly T independent value seen for

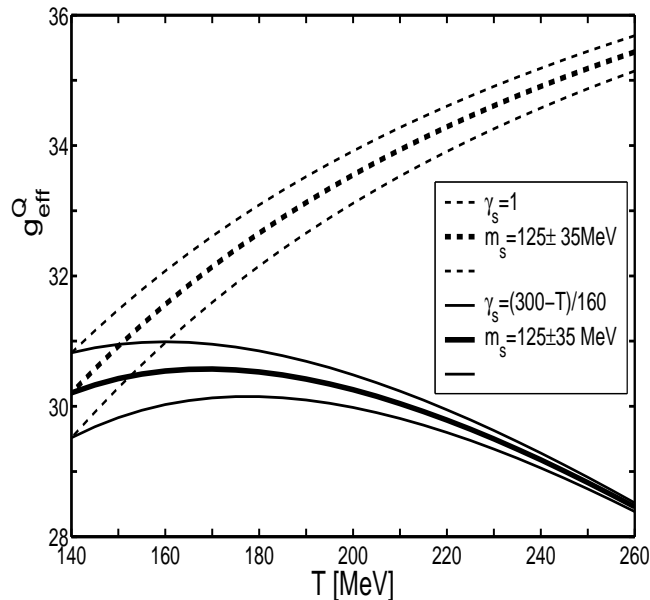


Figure 1. The Stefan-Boltzmann degrees of freedom g_{eff}^Q as function of temperature T for $m_s = 125$ MeV (central thick lines), thin upper and lower lines for $m_s = 90$ and 160 MeV respectively. The dashed lines are for chemically equilibrated u , d , s and G QGP plasma, with perturbative corrections for degeneracy. The solid lines are for QGP in which strangeness contents is increasing as temperature is decreasing, approaching chemical equilibrium.

for $T < 260$ MeV in Fig. 1, $g_{\text{eff}}^Q \simeq 30$ near to QGP breakup condition, which value is decreasing to $g_{\text{eff}}^Q \simeq 28$ for a hot QGP [2].

To quantify the strangeness enhancement signature due to deconfinement we compare in Fig. 2 the value of s/S in chemically equilibrated hadron matter with that of chemically equilibrated QGP, see Fig. 2, as function of chemical freeze-out temperature T . This figure quantifies the specific strangeness enhancement of the QGP phase. This enhancement implies in fast hadronization that a chemical nonequilibrium must arise among (strange) hadrons formed. The high density of strangeness present at QGP hadronization can therefore lead to a considerable enhancement of the yields of multi-strange antibaryons, and ϕ [6]. Strangeness enhancement is best expressed by the magnitude of γ_s/γ_q after hadronization, which we evaluate conserving strangeness and entropy. at hadronization, beginning with a QGP phase which is nearly chemically equilibrated at the point of hadronization:

$$s/S = f(\gamma_s, \gamma_q, T) \simeq (\gamma_s/\gamma_q)^{5/6} (0.026 \pm 0.01), \quad T \in (140, 180) \text{ MeV}. \quad (3)$$

Only when one considers the entropy content as measured by hadron yields, the understanding of the strangeness production in QGP is reliable. If instead the production of strangeness is studied at some presumed ‘hydro’-inspired space-time profile of temperature T , results are meaningful only if the QGP entropy S content has been directly related to an observed hadron multiplicity. Namely, if the initial temperature is modeled to be 20% below value needed for the observed entropy, the

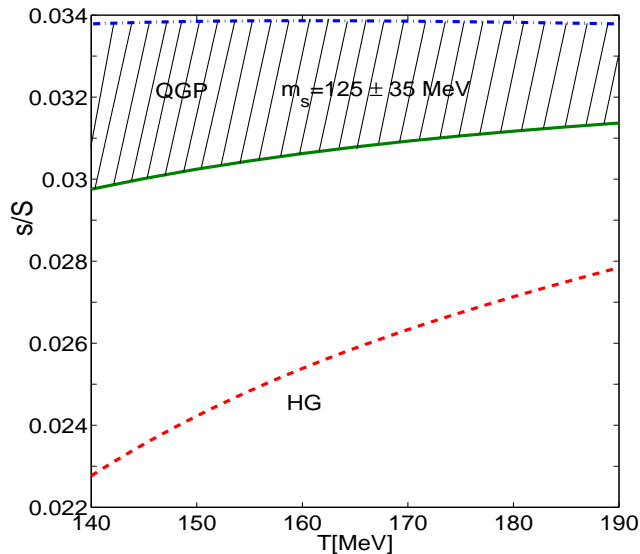


Figure 2. Strangeness to entropy ratio $s/S(T; \mu_B = 0, \mu_S = 0)$ for the chemically equilibrated QGP (green, solid line for $m_s = 160$ MeV, blue dash-dot line for $m_s = 90$ MeV); and for chemically equilibrated HG (red, dashed).

initial entropy content is cut in half. In the QGP this means that there are half as many gluons, and the rate of strangeness production by gluon fusion is cut down by a factor 4, which in turn implies that strangeness would not equilibrate in QGP.

3. Energy Scan at CERN-SPS

We analyze the particle production obtained in the energy scan of the NA49 experiment at CERN-SPS [3], and also include the results of our earlier analysis of the top AGS data [7]. The outcome of the fit procedure is stated in the top section of table 1. The λ_s values, marked with an asterix * in table 1, are result of a strangeness conservation constraint, which, however, is not chosen to be zero, but as shown in table: since strangeness conservation constraint involves several particle yields it is inappropriate to insist on $s - \bar{s} = 0$, since this correlates the errors of the input data which are experimentally not correlated. Our procedure was to fit first without strangeness conservation, and once we see the strangeness asymmetry to fix it at the best value shown in table so that the resulting procedure of fixing λ_s is the same as used by other groups, but that there is no unnecessary error constraint introduced among strange hadrons.

It is important to inspect the profiles of χ^2 , and of the confidence level $P[\%]$ determining the fit quality, see Fig.3. We observe that the results for AGS 11.6 and SPS 20 GeV differ from the remainder of the SPS results (30, 40, 80 and 158 GeV) in the outcome of the fit. The low energy results, obtained at two different experimental locations, clearly favor a value of $\gamma_q < 1$, combined with relatively large

Table 1. For each projectile energy E [AGeV] for AGS and SPS energy range, we present in the header $\sqrt{s_{\text{NN}}}$, the invariant center of momentum energy per nucleon pair, y_{CM} the center of momentum rapidity. This is followed by statistical parameters T, λ_i, γ_i obtained in the fit, the strangeness asymmetry required, and we present the resulting chemical potentials μ_B, μ_S , the reaction volume V and the centrality of the reaction considered. This is followed first by input and than by output total hadron multiplicity $N_{4\pi}$.

E [AGeV]	11.6	20	30	40	80	158
$\sqrt{s_{\text{NN}}}$ [GeV]	4.84	6.26	7.61	8.76	12.32	17.27
y_{CM}	1.6	1.88	2.08	2.22	2.57	2.91
T [MeV]	157.8±0.7	153.4±1.6	123.5±3	129.5±3.4	136.4±0.1	136.4±0.1
λ_q	5.23±0.07	3.49±0.08	2.82±0.08	2.42±0.10	1.94±0.01	1.74±0.02
γ_q	0.335±0.006	0.48±0.05	1.66±0.10	1.64±0.04	1.64±0.01	1.64±0.001
γ_s	0.190±0.009	0.38±0.05	1.84±0.32	1.54±0.15	1.54±0.05	1.61±0.02
λ_{I3}	0.877±0.116	0.863±0.08	0.939±0.023	0.951±0.008	0.973±0.002	0.975±0.004
λ_s	1.657*	1.41*	1.36*	1.30*	1.22*	1.16*
$s - \bar{s}/s + \bar{s}$	0	-0.092	-0.085	-0.056	-0.029	-0.062
μ_B [MeV]	783	576	384	344	271	227
μ_S [MeV]	188	139	90.4	80.8	63.1	55.9
V [fm ³]	3596±331	4519±261	1894±409	1879±183	2102±53	3004±1
$N_{4\pi}$ centrality	most central	7%	7%	7%	7%	5%
$R = p/\pi^+, N_W$	$R = 1.23 \pm 0.13$	349±6	349±6	349±6	349±6	362±6
Q/b	0.39±0.02	0.394±0.02	0.394±0.02	0.394±0.02	0.394±0.02	0.39±0.02
π^+	133.7±9.9	184.5±13.6	239±17.7	293±18	446±27	619±48
$R = \pi^-/\pi^+, \pi^-$	$R = 1.23 \pm 0.07$	217.5±15.6	275±19.7	322±19	474±28	639±48
$R = K^+/K^-, K^+$	$R = 5.23 \pm 0.5$	40±2.8	55.3±4.4	59.1±4.9	76.9±6	103±10
K^-	3.76±0.47	10.4±0.62	16.1±1	19.2±1.5	32.4±2.2	51.9±4.9
$R = \phi/K^+, \phi$	$R = 0.025 \pm 0.006$	1.91±0.45	1.65±0.5	2.5±0.25	4.58±0.2	7.6±1.1
Λ	18.1±1.9	28±1.5	41.9±6.1	43.0±5.3	44.7±6.0	44.9±8.9
$\bar{\Lambda}$	0.017±0.005	0.16±0.03	0.50±0.04	0.66±0.1	2.02±0.45	3.68±0.55
Ξ^-		1.5±0.13	2.48±0.19	2.41±0.39	3.8±0.260	4.5±0.20
Ξ^+			0.12±0.06	0.13±0.04	0.58 ±0.13	0.83±0.04
$\Omega + \bar{\Omega} // K_S$				0.14±0.07		81±4
$b \equiv B - \bar{B}$	375.6	347.9	349.2	349.9	350.3	362.0
π^+	135.2	181.5	238.7	290.0	424.5	585.2
π^-	162.1	218.9	278.1	326.0	461.3	643.9
K^+	17.2	39.4	55.2	56.7	77.1	109.7
K^-	3.58	10.4	15.7	19.6	35.1	54.1
K_S	10.7	25.5	35.5	37.9	55.1	80.2
ϕ	0.46	1.86	2.28	2.57	4.63	7.25
p	174.6	161.6	166.2	138.8	138.8	144.3
\bar{p}	0.021	0.213	0.68	0.76	2.78	5.46
Λ	18.2	29.7	39.4	34.9	42.2	48.3
$\bar{\Lambda}$	0.016	0.16	0.51	0.63	2.06	4.03
Ξ^-	0.47	1.37	2.44	2.43	3.56	4.49
Ξ^+	0.0026	0.027	0.089	0.143	0.42	0.82
Ω	0.013	0.068	0.14	0.144	0.27	0.38
$\bar{\Omega}$	0.0008	0.0086	0.022	0.030	0.083	0.16
$K^0(892)$	5.42	13.7	11.03	12.4	18.7	26.6
Δ^0	38.7	33.43	25.02	26.6	27.2	28.2
Δ^{++}	30.6	25.62	22.22	24.2	25.9	26.9
$\Lambda(1520)$	1.36	2.06	1.73	1.96	2.62	2.99
$\Sigma^-(1385)$	2.51	3.99	4.08	4.26	5.24	5.98
$\Xi^0(1530)$	0.16	0.44	0.69	0.73	1.14	1.44
η	8.70	16.7	19.9	24.1	38.0	55.2
η'	0.44	1.14	1.10	1.41	2.52	3.76
ρ^0	12.0	19.4	14.0	18.4	32.1	42.3
$\omega(782)$	6.10	13.0	10.8	15.7	27.0	38.5
$f_0(980)$	0.56	1.18	0.83	1.27	2.27	3.26

V, T , while the higher energy data favor $\gamma_q \rightarrow \gamma_q^{\text{cr}}$. The recently reported enlarged set of NA49 experimental results help to discriminate the chemical hadronization condition.

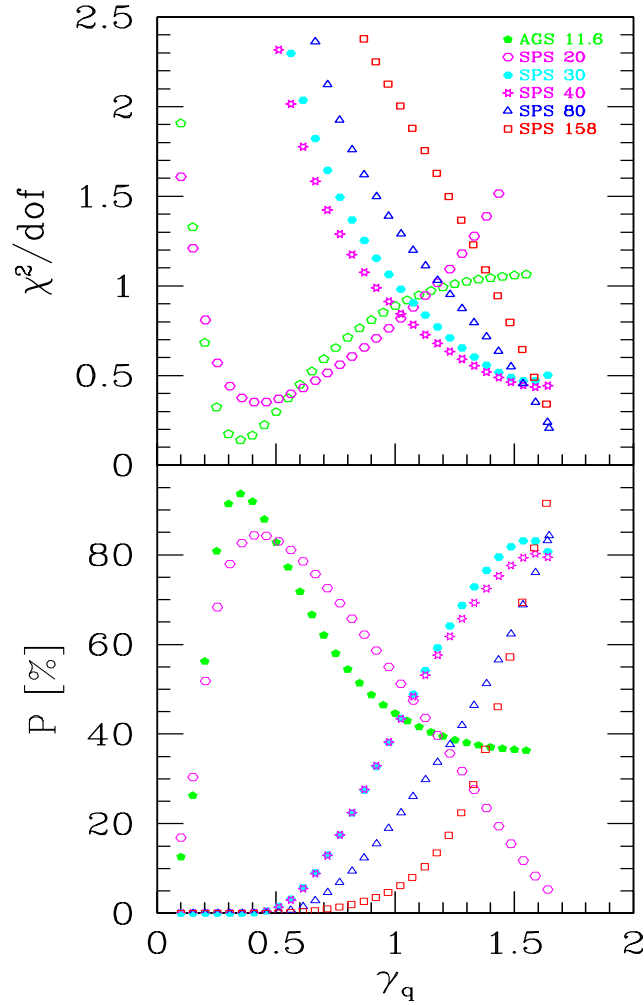


Figure 3. χ^2/dof (top) and the associated confidence level P [%] (bottom) as function of γ_q , the light quark phase space occupancy, for the AGS/SPS energy range.

Inspecting, in particular, the 80 and 158 GeV profiles, presented in Fig. 3, we recognize that the semi-equilibrium model with $\gamma_q = 1$ has a comparatively low viability compared to the full chemical non-equilibrium model we advance.

The SHARE package offers the opportunity to evaluate the physical properties of the fireball in its local frame of reference: since we look at the hadron yields, the flow velocity information is not retained. These results are shown in table 2. We note that the chemical freeze-out at low energy (AGS 11.6 and SPS 20 GeV) occurs from a much more dilute physical state, the energy density of the high energy (30, 40, 80 and 158 GeV) data points hovers well above 400–500 MeV/fm³, about a factor 2.5 higher than at low energy. We further note that between 20 and 30 GeV the ratio E/T_S shifts from a value below unity to above unity as required for the sudden, supercooled hadronization mechanism for $E > 20$ A GeV. There is a steady growth in the yield of strangeness, both measured in terms of s/S as well as the yield per participant (net baryon number b). There is a decrease in the energy retained, indicating that the flow effects grow rapidly,

Table 2. The physical properties. Top: pressure P , energy density $\epsilon = E_{\text{th}}/V$, entropy density S/V , for AGS and CERN energy range at, (top line) projectile energy E [GeV]; middle: dimensionless ratios of properties at fireball breakup, E_{th}/TS ; strangeness per entropy s/S , strangeness per baryon s/b ; and bottom the fraction of initial collision energy in thermal degrees of freedom, $(2E_{\text{th}}/b)/\sqrt{s_{\text{NN}}}$, the energy cost to make strangeness pair E_{th}/\bar{s} , thermal energy per hadron at hadronization E_{th}/h .

$E[\text{AGeV}]$	11.6	20	30	40	80	158
$\sqrt{s_{\text{NN}}} [\text{GeV}]$	4.84	6.26	7.61	8.76	12.32	17.27
$P[\text{MeV}/\text{fm}^3]$	21.9	21.3	58.4	68.0	82.3	76.9
$\epsilon[\text{MeV}/\text{fm}^3]$	190.1	166.3	429.7	480.2	549.9	491.8
$S/V[1/\text{fm}^3]$	1.25	1.21	2.74	3.07	3.54	3.26
E_{th}/TS	0.96	0.92	1.27	1.20	1.14	1.11
$100\bar{s}/S$	0.788	1.26	1.94	1.90	2.16	2.22
\bar{s}/b	0.095	0.202	0.289	0.314	0.459	0.60
$(2E_{\text{th}}/b)/\sqrt{s_{\text{NN}}}$	0.752	0.722	0.612	0.589	0.536	0.472
$E_{\text{th}}/\bar{s} [\text{GeV}]$	19.25	10.9	8.08	8.21	7.19	6.80
$E_{\text{th}}/h [\text{GeV}]$	1.33	1.18	0.866	0.859	0.827	0.766

pushing the fraction of energy stopping below 50% at the top SPS energy. The cost of strangeness pair production E_{th}/\bar{s} decreases, as does the energy per hadron produced E_{th}/h . Both these quantities use energy content in the local rest frame, and thus do not include the kinetic energy of matter flow at hadronization, which originated from the thermal pressure, which has driven the expansion matter flow.

4. Discussion of Results

At the top SPS energy, the value of $s/S = 0.022$ implies for a QGP source a $\gamma_s^Q \simeq 0.7$, which corresponds to $\gamma_s/\gamma_q \simeq 1$. This, in fact, is the reason why chemical equilibrium $\gamma_q = \gamma_s = 1$ ‘marginally works’ for this data set. However, as function of energy we see a very spectacular preference for non-equilibrium, of two different types. For two lowest reaction energies considered, we are below chemical equilibrium and for other, higher energies, with $\sqrt{s_{\text{NN}}} > 7.6$ GeV we see over saturation of chemical occupancies.

Since we fit data very well, we also describe precisely the K^+/π^+ ratio as we show in Fig. 4. The maximum of the ratio K^+/π^+ occurs for $E = 30$ A GeV where we find $\gamma_i > 1$. An anomaly associated with the horn is the large yield of Λ , and protons, see bottom section of table 1. We further note that the structure of the horn shown by dashed (semiequilibrium) and dotted (equilibrium) lines is also reproduced qualitatively, contrary to reports made by other groups. We have traced this behavior to our relaxation of the strangeness conservation condition.

Do the low energy results imply absence of quark matter, and thus reactions between

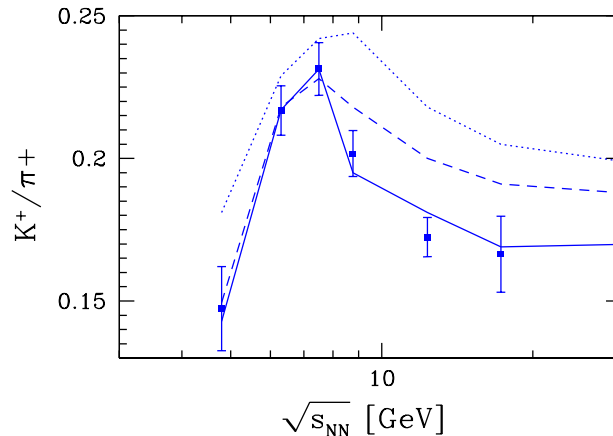


Figure 4. K^+/π^+ total yields as function of $\sqrt{s_{NN}}$. The solid lines show chemical non-equilibrium model fit. The chemical equilibrium fit result is shown by the dotted line. The dashed line arises finding best γ_s for $\gamma_q = 1$.

individual hadrons? Our analysis shows that the chemical freeze-out occurs in a highly dilute phase. However, the rapid rise of strangeness yield as function of reaction energy, suggests that the strangeness production processes differ from those encountered in normal hadron matter. For this reason we favor a constituent quark matter reaction picture at 11.6 and 20 A GeV, with color deconfinement arising yet below this energy range. The relatively high temperature and low γ_q are consistent with properties of constituent quark phase with $m_{u,d} \simeq 340$ MeV and $m_s \simeq 500$ MeV, gluons are ‘frozen’. In such a massive deconfined quark phase chiral symmetry is not restored. For $\mu_B \rightarrow 0$ the lattice results unite the chiral symmetry restoration, in which $m_q \rightarrow 0$, with the deconfinement transition.

In Summary: the physical properties we find for the hadronization of 30, 40, 80, 158 A GeV most central heavy ion reactions correspond to the expected behavior of the chirally symmetric QGP phase. SHM model described these results well, hadron simulations (not discussed here) fail to account for multistrange (anti)baryons.

Acknowledgments Work supported by a grant from: the U.S. Department of Energy DE-FG02-04ER4131. LPTHE, Univ. Paris 6 et 7 is: Unité mixte de Recherche du CNRS, UMR7589 .

- [1] J. Letessier and J. Rafelski, arXiv:nucl-th/0504028.
- [2] I. Kuznetsova and J. Rafelski, Eur. Phys. J. C **51** (2007) 113 [arXiv:hep-ph/0607203].
- [3] The results of NA49 we use were provided by M. Gazdzicki and B. Lungwitz, (private communication, September 2006)
- [4] G. Torrieri et.al. Comput. Phys. Commun. **167** (2005) 229 [arXiv:nucl-th/0404083]; ibid **175** (2006) 635 [arXiv:nucl-th/0603026].
- [5] P. Koch et.al. Nucl. Phys. A **444** (1985) 678 and Phys. Rept. **142** (1986) 167.
- [6] J. Rafelski, Phys. Rept. **88** (1982) 331.
- [7] J. Letessier, J. Rafelski and G. Torrieri, arXiv:nucl-th/0411047.